Available online at www.sciencedirect.com
ScienceDirect
Cement and Concrete Research 37 (2007) 909 – 915
Cement and Concrete Research

Permeability characteristics of carbonated concrete considering capillary pore structure

Ha-Won Song *, Seung-Jun Kwon

Department of Civil Engineering, Yonsei University, Seoul, 120-749, Republic of Korea

Received 2 April 2005; accepted 21 March 2007

Abstract

During carbonation process, the calcium phases present in cement are attacked by CO_2 and converted into $CaCO_3$ and the permeability of concrete is changing due to the change in porosity. The rate of carbonation depends upon porosity and moisture content of the concrete. Especially in underground reinforced concrete structures, the interior portion of concrete surface may be exposed to carbonation and the exterior portion of concrete surface exposed to wet soil or underground water. As carbonation proceeds from outer surface into internal portion of concrete, microstructure is also changed continuously from outer surface into internal portion of concrete. Even the deteriorations in the structures due to the carbonation have been reported more, research on permeability characteristics of concrete considering carbonation and micro-structural information is very scarce.

In this study, the permeability coefficient in carbonated concrete is derived by applying a capillary pore structure formation model in carbonated cement mortar and assuming that aggregates do not affect carbonation process in early-aged concrete as a function of porosity. The permeability obtained from the micro-level modeling for carbonated concrete is verified with the results of accelerated carbonation test and water penetration test in cement mortar.

Keywords: Concrete; Carbonation; Permeability; Capillary pore structure; Durability modeling

---

1. Introduction

The porous structure of concrete permits the ingress of CO_2, chloride, O_2 and moisture into the concrete leading to corrosion of reinforcing bars. The permeability of concrete, which is mainly dependant on permeability characteristics of cement paste, can be a major factor affecting the durability of concrete because aggressive agents penetrate through porous concrete more rapidly [1]. Thus a model which can simulate behavior of both moisture transfer in early aged concrete and deterioration process in hardened concrete has been introduced for the analysis of durability resistance of the concrete. Permeability coefficient of concrete can be a good index to evaluate the durability resistance of concrete and it can be obtained by both laboratory as well as field studies [2]. In underground reinforced concrete (RC) structures, the exterior surface of concrete is exposed to wet soil or underground water and so the carbonation is very slow due to low diffusivity and CO_2 concentration, but interior surface is exposed to higher diffusivity and CO_2 concentration so that the carbonation is more rapid.

1.1. Effect of carbonation on porosity

The pH of pore water inside carbonated concrete is decreased due to intrusion of CO_2, which may lead to corrosion of rebar in carbonated concrete. During the carbonation process, the volume of hydrates increased up to about 11.7% and the porosity is decreased to certain extent [3]. The characteristic changes in carbonated concrete are summarized with change in weight, moisture absorption [4], surface tension in pore water [5], CO_2 diffusivity [3,5,6], and moisture saturation [7]. These factors are mainly dependent on change in capillary pore structure due to consumed hydrates and $CaCO_3$ formation. These factors were considered for simulation modeling of carbonation process and coupled deterioration with chloride attack [3,8,9].

---

* Corresponding author. Tel.: +82 2 21232806; fax: +82 2 364 5300.
E-mail address: song@yonsei.ac.kr (H.-W. Song).

0008-8846/$ - see front matter © 2007 Elsevier Ltd. All rights reserved.
doi:10.1016/j.cemconres.2007.03.011

It is well known that carbonation, a consequence of the transformation of $Ca(OH)_2$ to $CaCO_3$ causes variation of the microstructure of mortars and concretes by decreasing their porosity. Carbonation also causes the change in material properties that are closely related to the microstructure, such as permeability, diffusivity of gases, capillarity etc. Several authors have studied the variation of natural properties with carbonation process. Ngala [10] investigated the effects of carbonation on pore structure and diffusion properties of hydrated cement pastes and found that there was a reduction in the total porosity of the three cement systems (Ordinary Portland cement, fly ash and slag pastes) with carbonation, but a redistribution of the pore sizes; the proportion of large capillary pores (diameter >30 nm) was increased slightly for the OPC pastes but much more significantly for the fly ash and slag pastes. Bier [11] investigated the effect of carbonation on the pore structure of cementitious systems that were manufactured with different types of cement. It was found that, for cements with high clinker content, carbonation led to a considerable reduction of the capillary pore volume, whereas for cements with a slag content exceeding approximately 50% by mass, a coarser capillary pore system was formed during carbonation. This was attributed to a considerable decomposition of the CSH gel in these cement pastes. Johannesson and Utgenannt [12] studied the change of specific surface area of cement mortar using BET theory. Holly et al. [13] discussed the variations of different properties like permeability, porosity and micro pore structure distribution as a consequence of the carbonation process in cement based materials.

It is also reported that carbonation often reduces the capillary porosity of the cement paste matrix in cover concrete [14–16]. The permeability of the cover concrete would be expected to change with carbonation in parallel to the changes of capillary porosity. Saeki et al. [17] studied the change in micro-structure of concrete due to carbonation and reported that the change in pore volume and pore size distribution due to carbonation depends on water–cement ratio and initial curing period. Pore volume in the carbonated portion is decreased in the case of the continuous carbonation test and also denseness of structure induced by carbonation affects the subsequent carbonation process.

The permeability in porous media like concrete is generally obtained as a function of porosity through experiment or capillary pore structure modeling [18]. Recently, the modeling of permeability is attempted for cracked concrete [19,20], concrete made with major mineral admixtures, and for concrete subjected to loading [21]. Studies on permeability of hardened concrete have generally been experimentally attempted with the assumption that the porosity is constant. The study of permeability of early-aged concrete by modeling capillary pore structure formation for varying early-aged porosity is very much limited and porosity change due to the carbonation is also considered to be very less.

In this study, a permeability modeling in mortar is carried out using the capillary pore structure formation model with consideration of the porosity change in cement paste during the carbonation process. The capillary pore structure formation in early-aged concrete becomes almost constant after 28 days, but it is changing due to carbonation under long term exposure conditions. A permeability modeling for concrete sections having different permeation layers which are changing with the carbonation was carried out and the model was verified through both accelerated carbonation test and water penetration test.

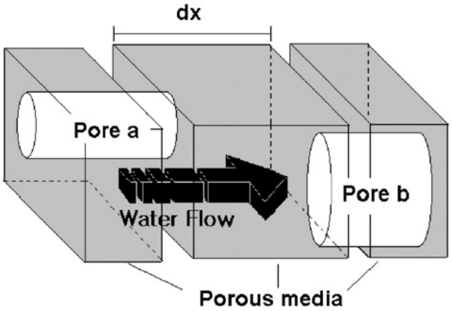

Fig. 1. Moisture flow through porous media.

2. Permeability modeling based on capillary pore structures

2.1. Pore size distribution and permeability modeling

Most of the important properties of hardened concrete are related to the quantity and characteristics of various types of pores in the cement paste and aggregate components of the concrete. The engineering properties of the concrete, such as strength, durability, shrinkage and permeability are directly influenced or controlled by the number, type and size of pores present [22]. It is believed that capillary voids 50 μm, referred to as macro pores, are detrimental to strength and impermeability, whereas voids smaller than 50 μm, referred to micro pores, are more related to drying shrinkage and creep [23].

The total porosity and pore size distribution are determined in advance to evaluate the permeability characteristics in porous media. The permeation capacity is influenced by the total porosity and the rate of transport is influenced by pore size distribution. Flow of moisture through porous media having pores is shown in Fig. 1.

The representative elementary volume (REV) is assumed to be connected with capillary pores assumed as each circular pipe and moisture flow across the REV, Q can be written as Eq. (1) in laminar flow state [24].

$$Q = -\left(\frac{1}{8\eta}\int_0^{\infty} r_i^2 \Omega_i \mathrm{d}r_i\right)\frac{\mathrm{d}P}{\mathrm{d}x} \tag{1}$$

where η is fluid viscosity, Ω_i is average area distribution function of pore i exposed on any arbitrary face cut perpendicular to the flow, r_i is pore radius, $\mathrm{d}P/\mathrm{d}x$ is fluid pressure gradient. Considering equivalent pore radius, r_{eq}, Eq. (1) can be written as Eq. (2) in Fig. 1 with representative pore radius r_{a} and r_{b}.

$$Q = -\left(\frac{1}{8\eta}\int_0^{\infty}\int_0^{\infty} C\cdot r_{\mathrm{eq}}^2 \mathrm{d}A_{\mathrm{a}}\mathrm{d}A_{\mathrm{b}}\right)\frac{\mathrm{d}P}{\mathrm{d}x} \tag{2}$$

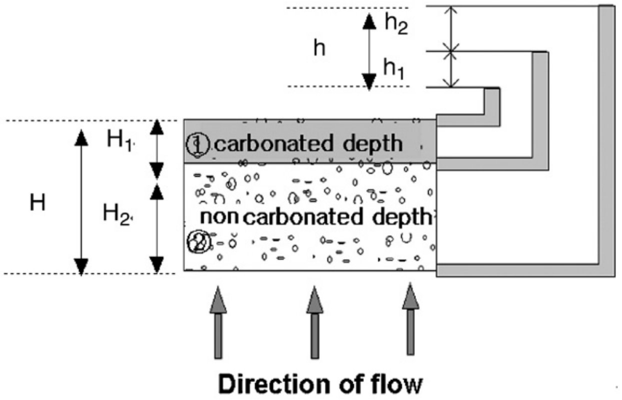

Fig. 2. Permeability in different permeable layer.

where r_{eq} is an equivalent pore radius, $\mathrm{d}A_i(=\Omega_i \mathrm{d}r_i)$ is pore area in pore i, C is constant. Intrinsic permeability can be written as Eq. (3) by comparing Eq. (2) with Darcy's Law.

$$k = \frac{C}{8}\left(\int_0^\infty r_{eq}\mathrm{d}A\right)^2 \tag{3}$$

Since the relationship between normalized volumetric porosity, dV and pore area, dA along with equivalent radius, r_{eq} can be written as Eq. (4), i.e., $\mathrm{d}V = n\mathrm{d}A/\phi_{total}$ where n is torturity factor ($=\pi^2/4$), the intrinsic permeability can be rewritten as Eq. (5) with total porosity, ϕ_{total}.

$$\mathrm{d}V = n\mathrm{d}A/\phi_{total} \tag{4}$$

$$k = \frac{C\phi_{total}^2}{8n^2}\left(\int_0^\infty r_{eq}\mathrm{d}V\right)^2 \tag{5}$$

Eq. (5) can be solved analytically if porosity distribution function is assumed. In this study, a porosity distribution function is utilized as a simplistic Reyleigh–Ritz function [24], Eq. (6) using the capillary pore structure formation model.

$$V = 1 - \exp(-Br), \quad \mathrm{d}V = Br\exp(-Br)\mathrm{d}\ln r \tag{6}$$

where V is fractional pore volume, B is parameter through micro pore structure model, r is pore radius. From Eqs. (5) and (6), Eqs. (7) and (8) can be obtained.

$$k = \frac{C\phi_{total}^2}{8n^2}\left(\int_0^\infty r \cdot Br\exp(-Br)\mathrm{d}r\right)^2 \tag{7}$$

$$k = \frac{C\phi_{total}^2}{8n^2}\left[\exp(-Br)\cdot\frac{(Br+1)}{B}\Big|_\infty^0\right]^2 \tag{8}$$

The intrinsic permeability function can be written finally as Eq. (9).

$$k = \frac{C\phi_{total}^2}{8n^2}\frac{1}{B^2} \tag{9}$$

Thus, the permeability, K in the Darcy's Law can be written as Eq. (10).

$$K = \frac{C\phi_{total}^2}{8n^2}\frac{1}{B^2}\cdot\frac{\rho g}{\eta} \tag{10}$$

where ρ (=999.3 kg/m^3) is fluid density, g (=9.81 m^2/s) is acceleration due to gravity, η ($=1794\times10^{-6}$ Pa s) [25]. The ϕ_{total} and B are total porosity and parameter derived from the multi-component hydration heat model and the capillary pore structure formation model, respectively [24], C is assumed as constant, 0.2.

2.2. Permeability modeling for carbonated concrete

The permeability model with different permeable layers can be explained as shown in Fig. 2. Let us consider the carbonated layer, H_1 and non-carbonated layer, H_2, the flow velocity is same for both layers and the total head loss is considered to be H_1+H_2 [21].

An equivalent permeability, K^{eq} in specimen, for multi-layer medium can be written as Eq. (11) from the Darcy's Law and total head loss can be written as Eq. (12).

$$K^{eq}\left(\frac{h}{H}\right) = K_1 i_1 + K_2 i_2 \tag{11}$$

$$h = H_1 i_1 + H_2 i_2 \tag{12}$$

where K_1 (m/s) and K_2 (m/s) are permeability in carbonated layer and in non-carbonated layer, i_1 and i_2 are each fluid pressure gradient for carbonated layer and non-carbonated layer, respectively.

From Eqs. (11) and (12), the equivalent permeability can be written as Eq. (13)

$$K^{eq} = \frac{H}{\frac{H_1}{K_1}+\frac{H_2}{K_2}} \tag{13}$$

By considering the permeability ratio (K_1/K_2) as A in Eq. (13), the permeability can be obtained as Eq. (14) with carbonation depth H_1.

$$K^{eq} = \frac{AH}{H_1 + (H - H_1)\cdot A}\cdot K_2 \tag{14}$$

From Eq. (10), it can be seen that the permeability in concrete is changed with direct proportion of square root of porosity, if the porosity in fully carbonated concrete is taken as 50% ratio of the non-carbonated concrete [26]. In this study, the permeability ratio A is assumed to be 0.25.

3. Permeability characteristics due to carbonation

3.1. Experimental program

In order to evaluate the permeability characteristics with carbonation, a water penetration test (WPT) is carried out as per

Table 1
Mix proportions of cement mortar specimens

W/C	Slump (cm)	Water (kg/m^3)	Cement (kg/m^3)	Sand (kg/m^3)
55	15	267	485	1353
65	15	267	410	1445

Table 2
Accelerated carbonation test conditions

CO_2 concentration	Temperature	R.H.	Exposed period	Intervals of measurement
5%	25±0.5 °C	65±5%	4 months	4 weeks

the previous work [19,27]. Cylindrical cement mortar specimens of size 10 cm. diameter and 20 cm height were cast and demoulded after 24 h and cured under water at 20 °C for 28 days. The WPT was carried out under non-carbonated condition after cutting the cement mortar slices of 10 cm height. Specimens with same mix proportions were prepared for an accelerated carbonation test after curing for 28 days and then the WPT was also carried out under carbonated condition. The accelerated carbonation test has been carried out over a period of 4 months. The mix proportions of mortar specimens are shown in Table 1 and the condition of accelerated carbonation test is shown in Table 2.

The schematic arrangement of WPT is shown in Fig. 3 and the water penetrating test set-up is shown in Fig. 4. The apparatus for the WPT consists of two plastic cells fitted in steel frame as shown in Fig. 3. The water head is kept as 30 cm and the water flow and head loss are measured.

In this study, the permeability coefficient is obtained by the Darcy's Law and the water flow in unit time can be explained by Eq. (15).

$$\frac{Q_\mathrm{f}}{\mathrm{d}t} = -\frac{A'\mathrm{dH}}{\mathrm{d}t} = K_\mathrm{p}\frac{HA}{L} \tag{15}$$

$$-\frac{\mathrm{d}H}{H} = K_p\frac{A\mathrm{d}t}{A'L} \tag{16}$$

where Q_f is total water flow, $Q_\mathrm{f}/\mathrm{d}t$ is flow rate, A is the area of cement mortar, A' is area of pipette attached to upside cell, L is thickness of specimen, K_p is permeability coefficient, H is water head. By integrating Eq. (16) from initial water head, H_0, to measured water head, H_1, as Eq. (16), the permeability coefficient K_p is obtained as Eq. (18).

$$-\int_{H_0}^{H_1}\frac{\mathrm{d}H}{\mathrm{d}t} = K_p\int_0^t\frac{A\mathrm{d}t}{A'L} \tag{17}$$

$$K_\mathrm{p} = \frac{A'L}{At}\ln\frac{H_0}{H_1} \tag{18}$$

As the specimen is partially dry during the initial stage of the WPT and water flow is not constant due to saturation and permeation so that the WPT is carried out in non-stationary condition. Thus, constant water flow and permeability coefficient can be obtained after full saturation of specimen with time.

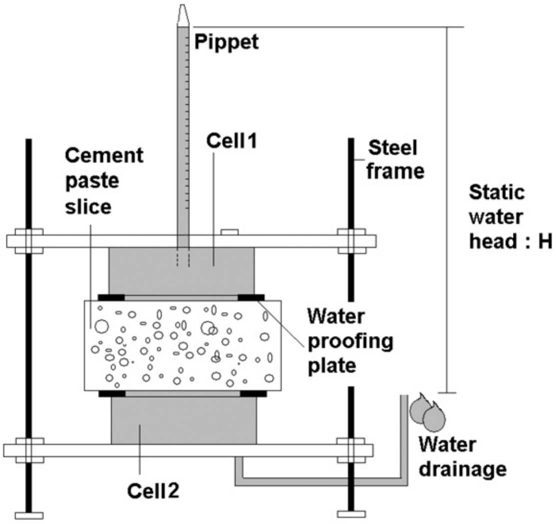

Fig. 3. Schematic arrangement of WPT.

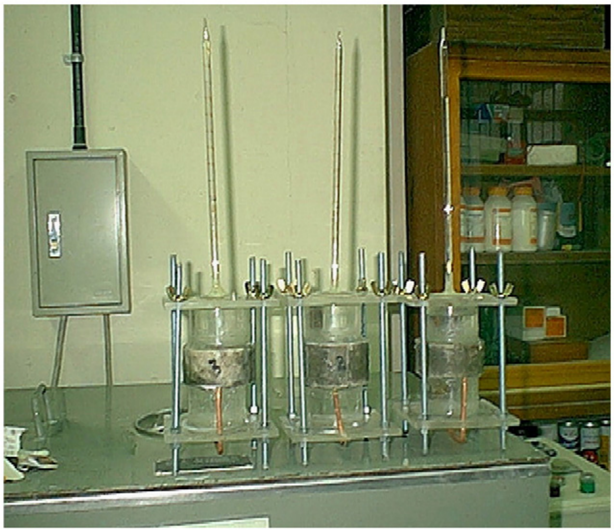

Fig. 4. WPT test set-up.

3.2. Experimental results and verification

3.2.1. Results of accelerated carbonation test

Core samples taken at different depths of the mortar specimens were cleaned and sprayed with a phenolphthalein indicator in

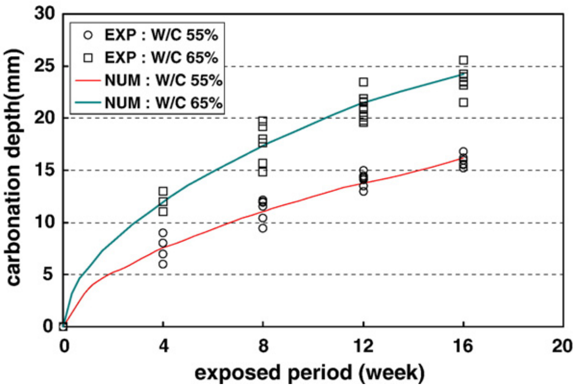

Fig. 5. Accelerated carbonation test results and analysis.

Table 3
Accelerated carbonation test results

W/C	N	Carbonation velocity $(mm/\sqrt{week})$	Correlation
55	32	3.98	0.933
65	32	6.05	0.938

order to test the alkalinity of the mortar specimens after accelerated carbonation test. The results of carbonation test are shown in Fig. 5 (Table 3).

From the figure it is observed that the carbonation depth increased with exposure period for both the water–cement ratios. The change in permeability of cement mortar due to carbonation in this is study utilized for FEM program [9] and the numerical results show that the prediction is comparably good with test results as shown in Fig. 5.

3.2.2. Evaluation of permeability coefficient

The permeability coefficient is decreased with time in non-stationary condition [19,21]. In this paper, the permeability coefficient is measured after 7–9 days from the water flow with Eq. (10), when the water flow is constant. The water flow and average permeability coefficient in non-carbonated specimen are shown in Fig. 6(a) and (b). From Fig. 6(b) it is observed that

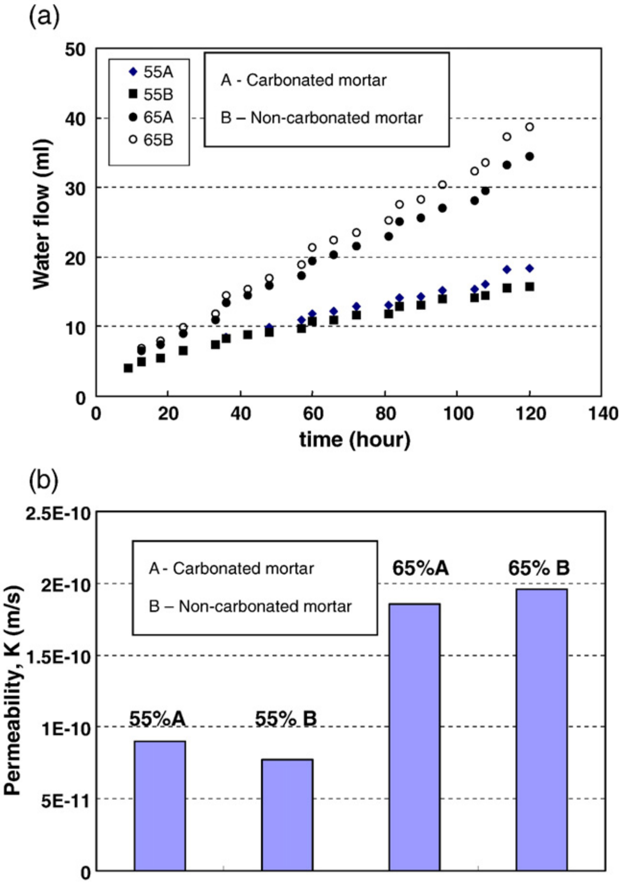

Fig. 6. (a) Water flow with time in non-carbonated mortar. (b) Average permeability coefficient in non-carbonated mortar.

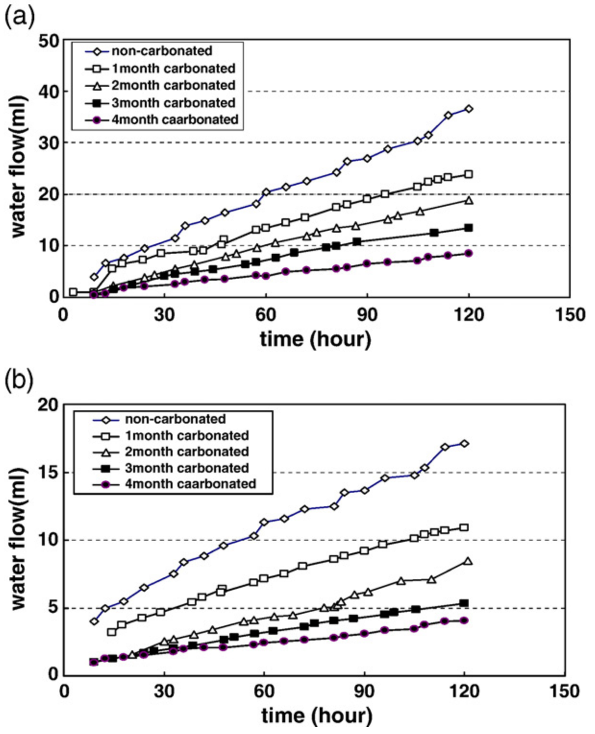

Fig. 7. Change in water permeability with time under carbonation. (a) Change in water permeability with time for carbonated mortar specimen (W/C: 65%). (b) Change in water permeability with time for carbonated mortar specimen (W/C: 55%).

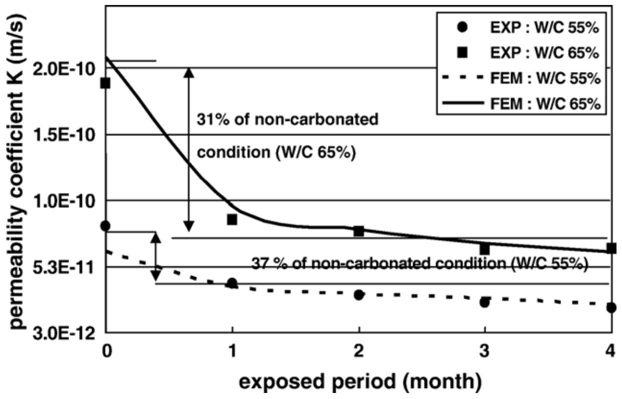

Fig. 8. Change in permeability coefficient with time under carbonation.

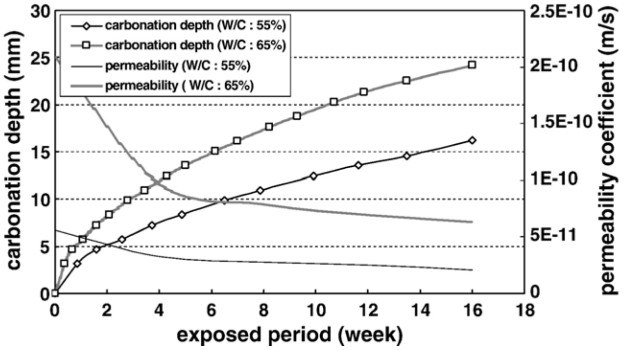

Fig. 9. Carbonation depth and change in permeability coefficient.

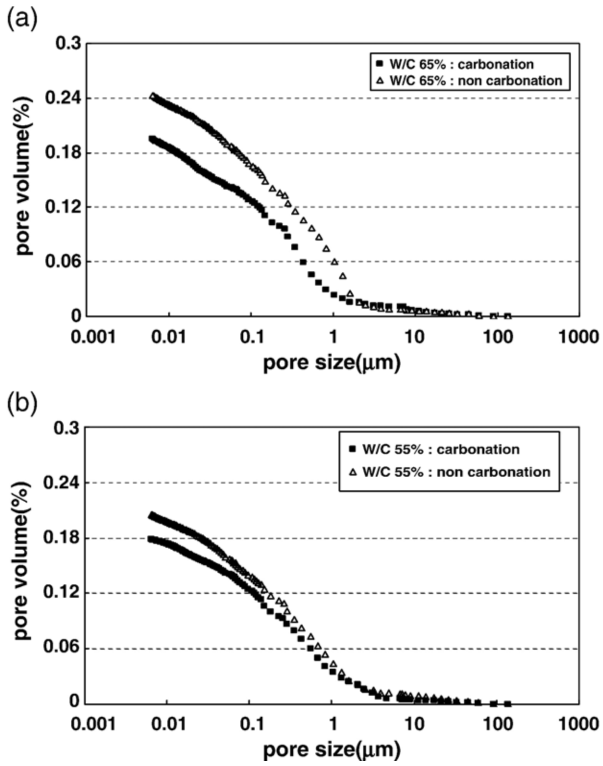

Fig. 10. Change in porosity of different W/C specimens. (a) Change in porosity of W/C 65% carbonated and non-carbonated specimens. (b) Change in porosity of W/C 55% carbonated and non-carbonated specimens.

the permeability coefficient is less for low W/C (0.55%) and higher for higher W/C (0.65%). The lesser W/C ratio showed lesser permeability coefficient, this is due to the reason that smaller and denser pore structure effect of the mortar. Russel and co-workers [28] also showed that the depth of carbonation and permeability primarily depends upon the water–cement ratio.

The change in water flow with time under carbonation with different W/C ratio is shown in Fig. 7. From the figure it is found that there is a linear increase in water flow observed with time and also the water flow is found to be less for highly carbonated concrete. The low W/C ratio (55%) mortar has lesser water flow than that with high W/C ratio mortar.

The permeability coefficient obtained from WPT is compared with analytical modeling and is shown in Fig. 8. As explained earlier, the permeability coefficient is decreased with direct proportion of square root of porosity. It decreases rapidly up to 1 month and then it reaches a steady state value after 4 months. In the non-carbonated cement mortar, the permeability coefficients measured are 1.9×10^{-10} m/s (65%), 8.35×10^{-11} m/s (55%), and it is decreased to 6.61×10^{-11} m/s (65%), 2.18×10^{-11} m/s (55%) after 4 months of accelerated carbonated condition. The decrease in carbonation rate is found to be 0.35 (65%) and 0.26 (55%) from experimental results, 0.31 (65%) and 0.37 (55%) from the proposed model. Fig. 9 shows both the permeability coefficient and carbonation depth with time. The experimental result with W/C 65% and 4 month carbonation period shows slight increase in permeability coefficient, however, the proposed model predicts the permeability coefficient under carbonation reasonably.

3.2.3. Porosity of carbonated mortar

Porosity of carbonated and non-carbonated mortar using MIP test for W/C 55% and 65% is shown in Fig. 10(a) and (b). From the figure it is found that 25–30% decrease in porosity was observed between the two W/C ratios and carbonated and non-carbonated mortars.

4. Conclusions

The conclusions on permeability characteristics of carbonated concrete considering capillary pore structure are as follows.

1. In order to verify the permeability of carbonated concrete, the permeability of cement mortar is derived analytically using multi-component hydration heat model and capillary pore structure formation model in early age. The permeability coefficient derived is directly proportional to the square root of porosity.
2. The permeability coefficient of concrete under carbonation is also derived through the modeling for permeability of carbonated concrete using Darcy's Law.
3. The analytical results are verified with results of the accelerated carbonation test and water penetration test. The verification shows that the proposed model reasonably predicts the change in permeability of concrete under carbonation. Accelerated carbonation test and water penetration test are carried out and the results are verified with those of numerical analysis and it found that the experimental results well agree with the simulation results.
4. The rate of water flow is increased with increase in water–cement ratio due to change in pore structure under both carbonated and non-carbonated conditions.
5. There is a linear increase in water flow observed with time and also the water flow is found to be less for highly carbonated concrete.
6. Permeability increased with exposure period irrespective of the water–cement ratio.

Acknowledgment

Prof. Koichi Maekawa at the University of Tokyo is highly acknowledged for providing motivation and valuable comments. The authors would like to acknowledge the Infra-Structure Assessment Research Centre (ISARC) and a Centre for Concrete Corea, Korea for their financial support.

References

[1] P.K. Metha, P.J.M. Monteiro, Concrete: durability, Prentice-Hall Inc., Englewood Cliffs, New Jersey, 1993, pp. 113–167.
[2] J.H. Bunget, S.G. Millard, Testing of Concrete in Structures, Blackie Academic & Professional, 1996.
[3] T. Ishida, K. Maekawa, Modeling of pH profile in pore water based on mass transport and chemical equilibrium theory, Concr. Libr. JSCE 37 (2001) 151–166.

[4] T. Saeki, H. Ohga, S. Nagataki, Mechanism of carbonation and prediction of carbonation process of concrete, Concr. Libr. JSCE 17 (1991) 23–36.

[5] V.G. Papadakis, C.G. Vayenas, M.N. Fardis, Physical and chemical characteristics affecting the durability of concrete, ACI Mater. J. 8 (1991) 186–196.

[6] V.G. Papadakis, C.G. Vayenas, M.N. Fardis, Fundamental modeling and experimental investigation of concrete carbonation, ACI Mater. J. 88 (1991) 363–373.

[7] K. Xu, Structure of hardened cement-fly ash systems and their related properties, Licentiate Thesis, Publication P-92:7. Division of Building Materials, Chalmers University of Technology, Sweden, 1990.

[8] H.-W. Song, H.J. Kim, T.H. Kim, K.J. Byun, A micro-mechanics based corrosion model for the prediction of service life in reinforced concrete structure, The 2nd International Symposium for the Safety of Construction and Special Structures, The Corrosion Science Society of Korea, Seoul, 2004.

[9] S.J. Kwon, H.-W. Song, K.J. Byun, S.H. Lee, Analysis of carbonation behavior of cracked concrete in early age, J. KSCE 24 (2004) 1011–1012.

[10] V.T. Ngala, Effect of carbonation on pore structure and diffusional properties of hydrated cement pastes, Cem. Concr. Res. 27 (1997) 995–1007.

[11] T. Bier, Influence of Type of Cement and Curing on Carbonation Progress and Pore Structure of Hardened Cement Pastes in MRS Symposium Proceedings, vol. 85, 1987, pp. 123–134.

[12] B. Johannesson, P. Utgenannt, Microstructural changes caused by carbonation of cement mortar, Cem. Concr. Res. 31 (2001) 925–931.

[13] J. Holly, D. Hampton, M.D.A. Thomas, Modelling relationships between permeability and cement paste pore microstructures, Cem. Concr. Res. 23 (1993) 1317–1330.

[14] L.J. Parrot, Measurement and modeling of porosity in drying and cement paste, in micro structural development during hydration of cement, MRS Symp. Proc. 85 (1987) 91–104.

[15] R. Patel, L.J. Parrot, J. Martin, D. Killoh, Gradients of microstructure and diffusion properties of cement paste caused by drying, Cem. Concr. Res. 15 (1985) 343–356.

[16] J. Kropp, Influence of carbonation on the structure of hardened cement paste and water transport, Proceedings of Intennational Colloquium, Esslingen, 1983, pp. 153–157.

[17] T. Saeki, H. Ohga, S. Nagataki, Change in micro-structure of concrete due to carbonation, Concr. Libr. JSCE 18 (1991) 1–11.

[18] D. Breysse, B. Gerard, Modeling of permeability in cement-based materials: Part 1—uncracked medium, Cem. Concr. Res. 27 (1997) 761–775.

[19] S.S. Park, H.-W. Song, K.J. Byun, Model for chloride diffusivity and water permeability in cracked concrete, J. KSCE 21 (6-A) (2001) 915–924.

[20] B. Gerard, J. Marchand, Influence of cracking on the diffusion properties of cement-based materials Part 1: Influence of continuous cracks on the steady-state regime, Cem. Concr. Res. 30 (2000) 37–43.

[21] C.M. Aldea, M. Ghandehari, S.P. Shah, A. Karr, Estimation of water flow through cracked concrete under load, ACI Mater. J. 97 (2000) 567–575.

[22] L. Basheer, P.A.M. Basheer, A.E. Long, Influence of coarse aggregate on the permeation, durability and the micro structure characteristics of ordinary Portland cement concrete, Constr. Build. Mater. 19 (2005) 685–690.

[23] P.K. Mehta, P.J.M. Monteiro, Concrete Structure, Properties and Materials, vol. 2, Prentice Hall, New Jersy, 1993, p. 548.

[24] K. Maekawa, R. Chaube, T. Kishi, Modeling of Concrete Performance: Hydration, Microstructure Formation and Mass Transport, Routledge, London, 1999.

[25] Concrete Society, Permeability testing of site concrete—a review of methods and experience, Report of a Concrete Society Working Party, vol. 12, Kensington, London, 1985.

[26] B.M. Das, Principles of Geotechnical Engineering-Equivalent Hydraulic Conductivity in Stratified Soil, PWS Publishing Company, 1998.

[27] D. Ludirdja, R.L. Berger, F. Young, Simple method for measuring water permeability of concrete, ACI Mater. J. 86 (1990) 433–439.

[28] D. Russell, P.A.M. Basheer, G.I.B. Rankin, A.E. Long, Effect of relative humidity and air permeability on prediction of the rate of carbonation of concrete, Structures and Buildings 146 (3) (2001) 319–326.